Earthquake Design of Flexible Soil Retaining Structures

J.H. Wood

John Wood Consulting, Lower Hutt

2017 NZSEE Conference

ABSTRACT: Many soil retaining wall structures are restrained from outward sliding movements and because of this it may not be appropriate to use the Mononobe-Okabe (MO) method to estimate the earthquake induced pressures on them. This semi-rigid or stiff wall category includes bridge abutments, building basement walls and hydraulic structures associated with hydro-power and flood control.

In the present research, finite element analyses have been completed on cantilever walls that deform by both rotation about their base and flexure in the wall stem. The wall stiffness parameters have been varied to produce pressure distributions under earthquake and gravity loads for walls that vary from rigid to sufficiently flexible for the MO method to be applicable.

The paper summarises the results of these finite element studies. An example is presented to demonstrate how the results can be applied in the earthquake design of semi-rigid or stiff walls.

1 INTRODUCTION

It is usual to simplify the complex problem of the interaction of earthquake generated elastic waves in the soil with wall structures by assuming that the earthquake ground motions are equivalent to dynamic inertia forces acting in the backfill mass. Dynamic pressures on the wall can then be estimated by analysing the wall and backfill modelled as an elastic continuum or failure wedge subjected to both gravity and horizontal body forces. The pressures that develop are very sensitive to the elastic flexibility of the structural components of the wall and the ability of the wall to move outward (rotation or translation) because of either permanent deformations in the foundation soils or inelastic behaviour of the structure.

1.1 Wall deformation categories

The behaviour of wall structures during earthquakes can be broadly classified into three categories related to the maximum strain condition that develops in the soil near the wall. The soil may remain essentially elastic, respond in a significantly nonlinear manner or become fully plastic. The rigidity of the wall and its foundations will have a strong influence on the type of soil condition that develops.

Many low walls are of cantilever type construction. In this type of wall, lateral pressures from vertical gravity and earthquake forces will often produce sufficient displacement within the wall structure to induce a fully plastic stress state in the retained soil. In more rigid free-standing walls, such as gravity (e.g. reinforced earth and crib block walls) counterfort walls and building basement walls, a fully plastic stress state may develop as the result of permanent outward movement from sliding or rotational deformations in the foundation. In cases where significant nonlinear soil behaviour or a fully plastic stress state occurs in the soil during earthquake loading, the well-known Mononobe-Okabe, (MO) method (Mononobe and Matsuo, 1929) can be used to compute earthquake pressures and forces acting on the wall.

Retaining structures that are not free-standing or have rigid foundations (piles or footings on rock or stiff soil) may not displace sufficiently, even under severe earthquake loading, for a fully plastic stress state to develop in the soil backfill. Particular examples of these types of walls include; bridge

abutments that may be rigidly attached to the bridge superstructure or founded on piles, basement walls that are an integral part of a building on a firm foundation, and closed culvert or tank structures embedded in the ground. For many of these types of walls, the assumptions of the MO method are not satisfied, and pressures and forces are likely to be significantly higher than given by its application.

In some cases, the wall may be sufficiently rigid for the soil to remain elastic under combined earthquake and gravity loads. Theory of elasticity methods for estimating earthquake induced pressures on rigid walls have been presented previously by Wood, 1973. More generally, there will be sufficient deformation for nonlinear soil effects to be important or for wall pressures to be significantly lower than for a fully rigid wall. These intermediate cases or stiff walls are more difficult to analyse than the limiting cases of fully plastic or rigid elastic behaviour. The present paper addresses the issue of walls that are flexible but not sufficiently flexible for the MO assumptions to be valid (called stiff walls). The top deflection under gravity and earthquake loads of stiff walls is typically less than 0.3% of the wall height.

1.2 **Previous research**

Theory of elasticity solutions for cantilever fixed base walls that deform in flexure and for rigid walls that deform by base rotation were presented by Wood, 1973 and Wood, 1991 respectively. Veletsos and Younan, 1997 presented approximate theory of elasticity solutions for both these types of walls.

The finite element model used by Wood, 1973 for the flexural analysis of the fixed base wall is shown in Figure 1. Earthquake loading was represented by a static horizontal body force assumed to be uniform throughout the soil layer and have magnitude $C_o\gamma$, where C_o is an acceleration coefficient and γ the soil unit weight. Gravity loading was represented by a body force of magnitude γ acting in the vertical direction. The wall height was divided into 20 equal elements and the soil mass was divided into 29 elements along the length of the layer with a square mesh used for the six elements closest to the wall. Plane strain rectangular elements with a second order displacement field were used. The model was verified against the analytical theory of elasticity solution for a rigid smooth wall (Wood, 1973).

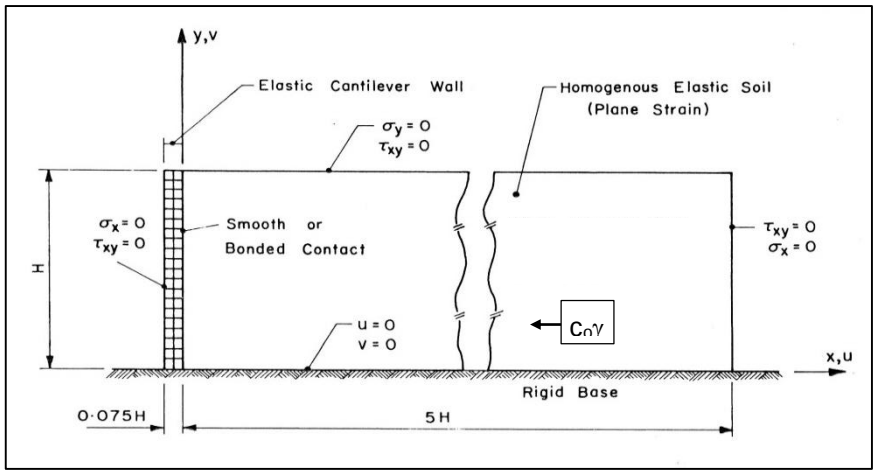

Figure 1. Finite element model for flexural analysis of cantilever wall.

Veletsos and Younan obtained analytical solutions for wall pressures by assuming that both the vertical normal stresses and the vertical displacements in the soil were zero. These assumptions limit the solution to the case when the soil is perfectly bonded to wall.

Both the previous Wood and Veletsos and Younan analyses assumed the soil to have uniform elastic properties with depth and only considered the case when tension was not eliminated from the pressure distribution near the top of the wall. Wood presented solutions for both a perfectly bonded contact between the soil and wall and a smooth wall. The Wood and Veletsos and Younan solutions based on elastic assumptions are an informative method of assessing the importance of the wall deformations and whether more refined nonlinear finite element analyses are necessary for stiff walls that have

intermediate flexibility.

2 ANALYSIS ASSUMPTIONS

Solutions more applicable to practical applications have been obtained in the present study for walls that deform by flexure in a cantilever stem and for rigid walls that rotate about their base using the Wood elastic finite element model shown in Figure 1 to analyse cases where tension in the normal pressure distribution acting on the wall is eliminated and to consider soils with both uniform and a linear increase of the elastic constants (shear modulus) from zero at the top of the wall to a maximum at the base.

Rectangular plain strain elements were used to model the soil, and beam elements to model the wall. A Poison's Ratio of 0.333 was assumed for the soil.

Results for the walls deforming in flexure are presented in terms of a flexibility parameter d_w defined by:

$$d_w = \frac{G\,H^3}{E_w I_w} \tag{1}$$

Where G is the average soil shear modulus, H the height of the retained soil layer, E_w is the Young's modulus for the wall I_w the second moment of area for wall.

Results for the walls deforming by rotation about the base are presented in terms of a flexibility parameter d_θ defined by:

$$d_\theta = \frac{G\,H^2}{R_\theta} \tag{2}$$

Where R_θ is the rotational stiffness of the base.

3 PRESSURE DISTRIBUTIONS

The normal pressure σ_x on the wall deforming in flexure under the horizontal earthquake load (uniform body force in the soil) in both the soil with uniform and linear with depth soil elastic constants and for smooth and bonded wall assumptions are shown in Figures 2 to 5. Corresponding pressure distributions for the rigid wall rotating about its base are shown in Figures 6 to 9. The pressure plots are presented in dimensionless parameters to enable them to be conveniently evaluated for any soil stiffness (shear modulus), soil unit weight, horizontal acceleration and wall height. For a given flexibility ratio d_w or d_θ, the normal pressures are dependent on the acceleration coefficient C_o, soil unit weight γ, and wall height H but are independent of the soil stiffness directly.

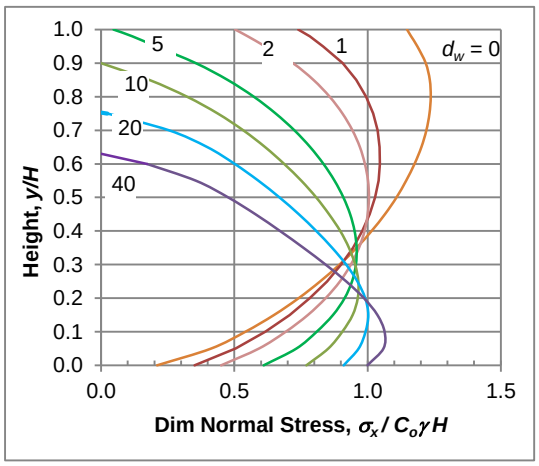

Figure 2. Flexure of smooth wall, uniform soil.

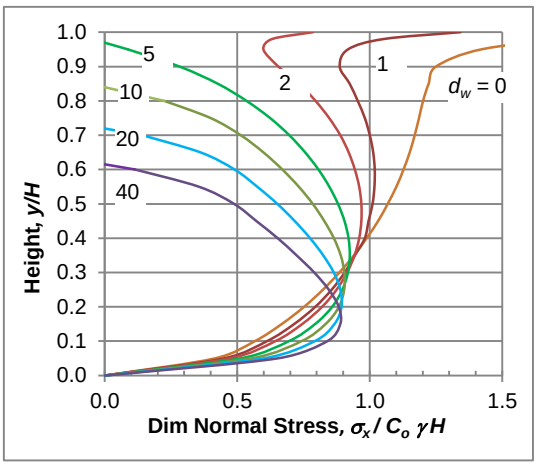

Figure 3. Flexure of bonded wall, uniform soil.

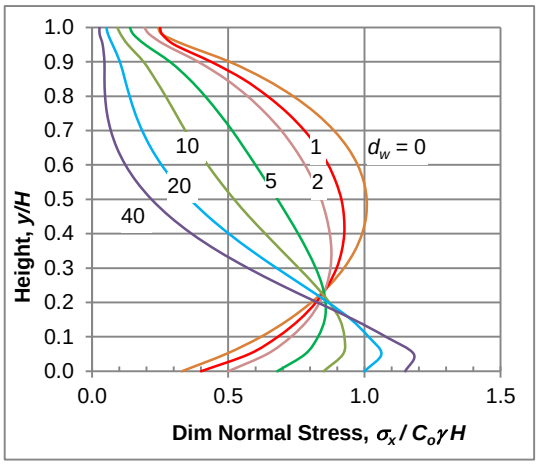

Figure 4. Flexure of smooth wall, linear soil.

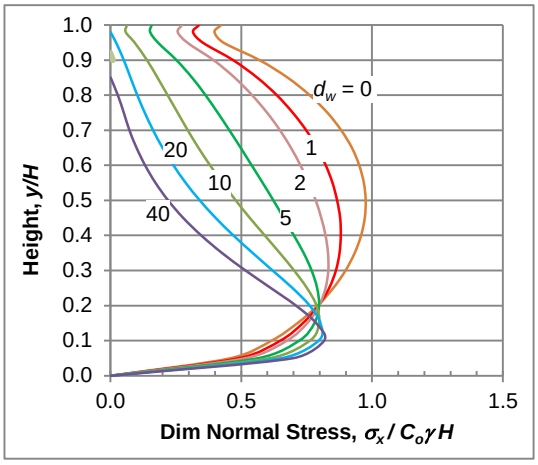

Figure 5. Flexure of bonded wall, linear soil.

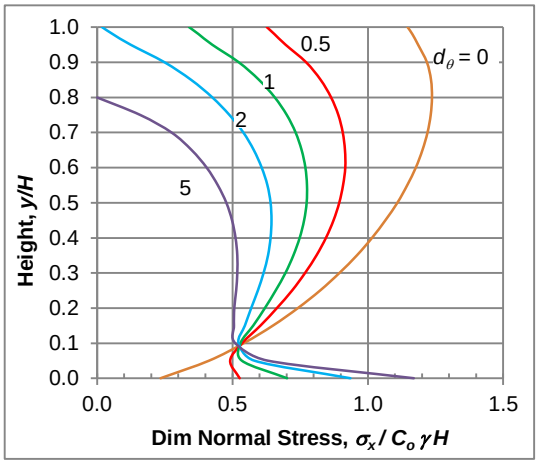

Figure 6. Rotation of smooth wall, uniform soil.

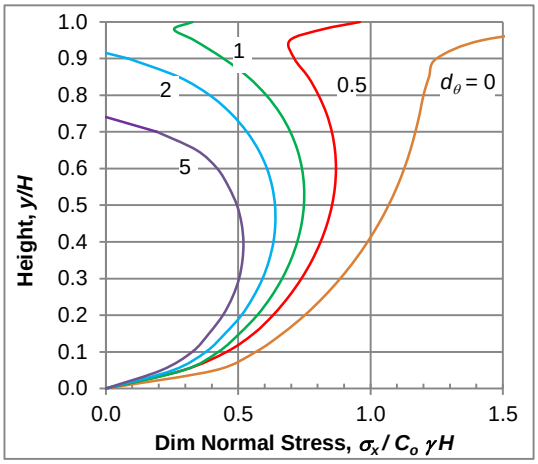

Figure 7. Rotation of bonded wall, uniform soil.

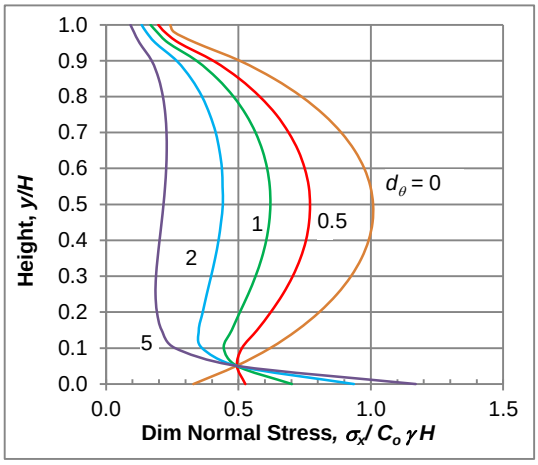

Figure 8. Rotation of smooth wall, linear soil.

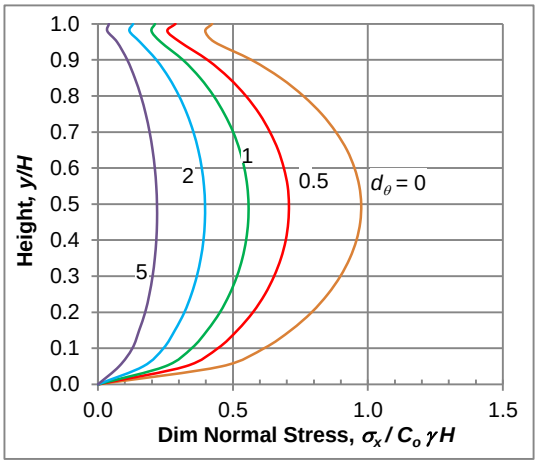

Figure 9. Rotation of bonded wall, linear soil

4 WALL BASE ACTIONS

The total force acting on the wall (or stem base shear) and the bending moment at the base of the wall were obtained by integrating the pressure distributions shown in Figures 2 to 9. Shears and moments for flexural deformation in smooth and bonded walls and for soil with uniform and linearly increasing elastic constants with depth are shown in Figures 10 and 11 respectively. The corresponding base force actions for the wall deforming by base rotation are shown in Figures 12 and 13.

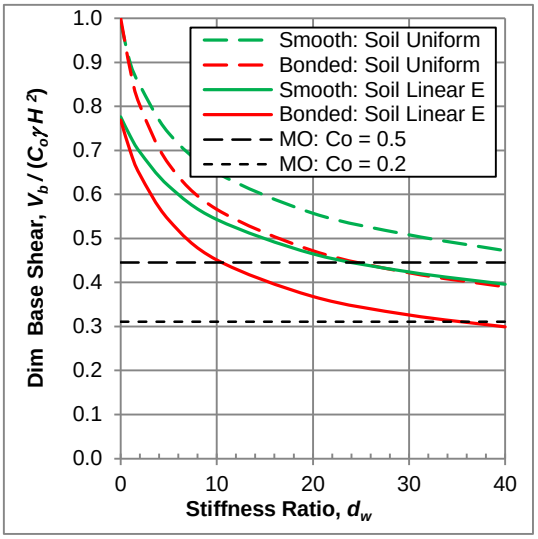

Figure 10. Base shear, flexural deformation.

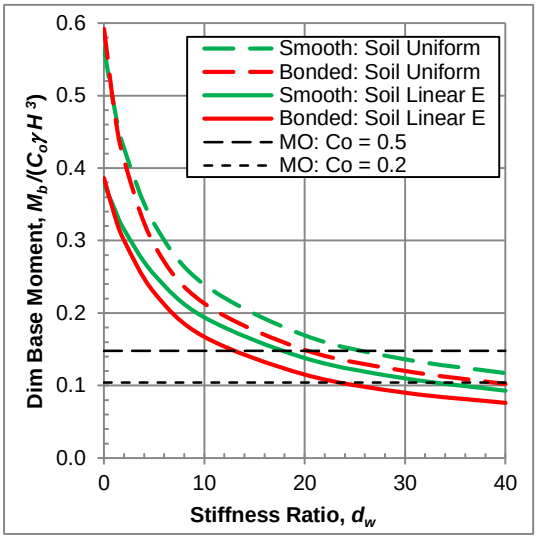

Figure 11. Base moment, flexural deformation.

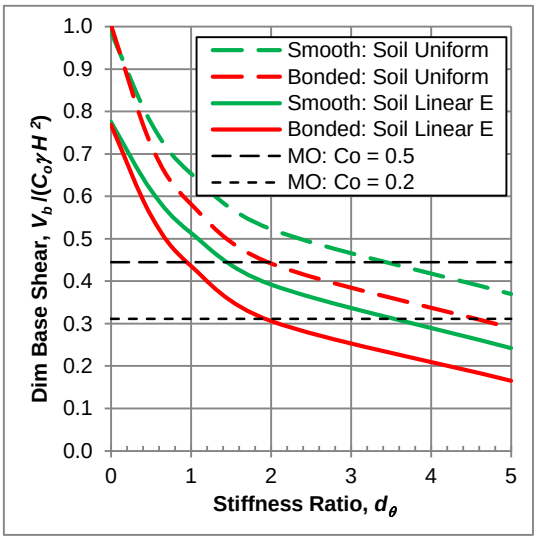

Figure 12. Base shear, rotational deformation.

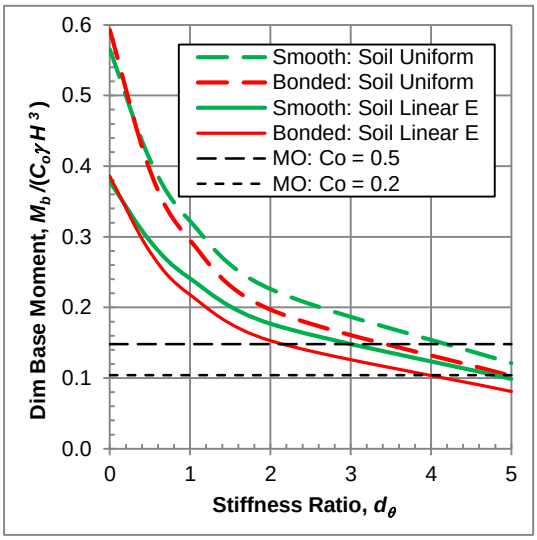

Figure 13. Base moment, rotational deformation.

The shears and moments shown in Figures 10 to 13 are plotted in dimensionless terms so that, as was the case for the normal pressures, they can be used to evaluate solutions for any values of C_o, γ and H. Superimposed on the plots are MO forces and moments calculated for a smooth wall assuming a soil friction angle $\phi = 35^o$. MO values are plotted for acceleration coefficient values of C_o = 0.2 and 0.5. Since the MO actions do not vary linearly with C_o and are independent of d_w and d_θ, they are drawn as separate horizontal lines over a range of typical C_o values used in design.

5 WALL DEFLECTIONS

Plots of the earthquake load displacement at the top of the wall, u_t for both smooth and bonded walls with uniform and linearly increasing elastic constants with depth are shown in Figure 14. The corresponding displacements for the wall deforming by base rotation are shown in Figures 15. The factor required to express the deflections in dimensionless form includes the soil shear modulus G in addition to Co, γ and H.

6 GRAVITY ACTIONS

In practical applications it is necessary to combine earthquake and gravity load pressures. Gravity

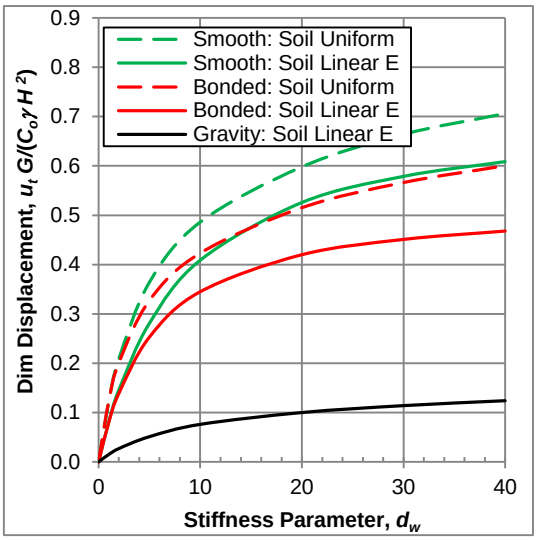

Figure 14. Top deflection, flexural deformation.

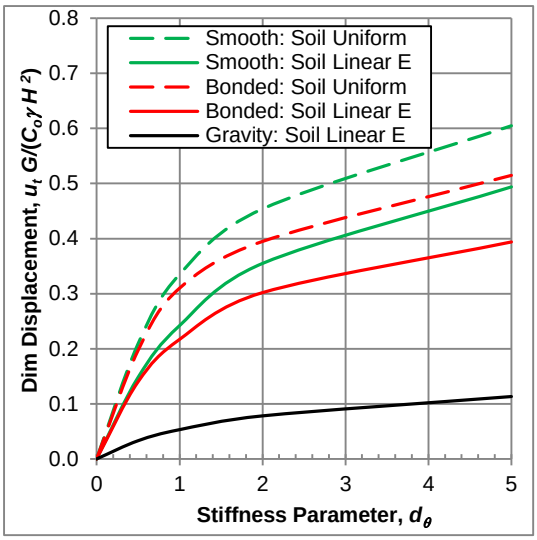

Figure 15. Top deflection, rotational deformation.

pressures for rigid walls can be calculated by the conventional at-rest assumption (pressure coefficient K_o = 1- sinϕ, where ϕ is the soil friction angle) or by assuming elastic theory which gives $K_o = \nu/(1-\nu)$ where ν is the soil Poison's ratio. For flexible walls, active Rankine pressure can be assumed but for stiff walls it is helpful to have results based on the elastic soil assumption consistent with the assumptions made for the earthquake pressures.

Gravity load shears and moments for flexural deformation in smooth and bonded walls and for soil with uniform and linearly increasing elastic constants with depth are shown in Figure 16. The corresponding base force actions for the wall deforming by base rotation are shown in Figure 17. Wall top deflections for the linear soil constants are shown in Figures 14 and 15. Deflections are approximately the same for both the linear and uniform soil assumptions.

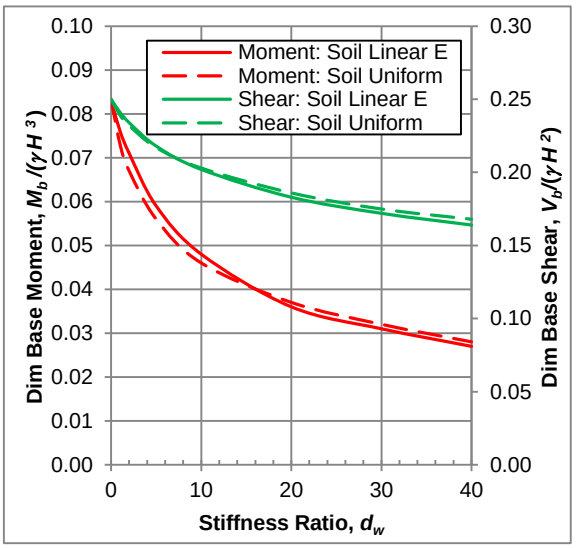

Figure 16. Gravity actions, flexural deformation.

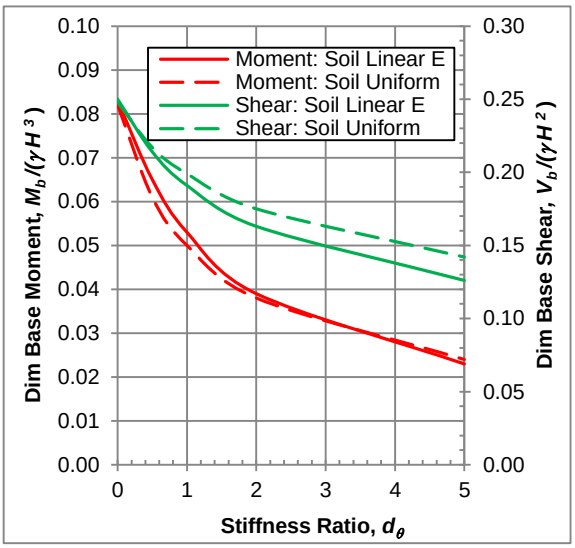

Figure 17. Gravity actions, rotational deformation.

7 STIFF WALL EXAMPLE

To illustrate the application of the results presented for the fixed base cantilever wall an analysis of a U-section flood control channel is presented below. The channel is based on the Wilson Canyon, San Fernando, California channel analysed by Wood, 1973. A typical section is shown in Figure 18. To simplify the example presented here, it was assumed that the main flexural steel was detailed so that the base section of the wall was the most critical section.

The assumed input parameters and a summary of the computed results are given in Table 1.

Table 1. Flood Control Channel Example

Parameter	Value	Comment
Input Parameters		
Wall stem height	3.0 m	
Stem thickness	0.25 m	
Cover to main reinforcement	50 mm	
Flexural reinforcement bar diameter	20 mm	
Flexural reinforcement bar spacing	250 mm	
Concrete strength, f_c	35 MPa	Assumed probable strength (25 x 1.4)
Reinforcement yield strength	300 MPa	Assumed probable strength (275 x 1.1)
Backfill unit weight, γ	19 kN/m^3	
Backfill friction angle	36^o	
Friction angle for wall face	0^o	Smooth wall. Low friction expected in strong shaking
Backfill ave Young's modulus, E	15 MPa	Linear: 0 at top increasing to maximum at base. Reduced to adjust for deformation from outward movement
Backfill soil Poisson's ratio, ν	0.333	
Backfill soil shear modulus, G	5.6 MPa	Calculated from E and ν: $G = E/(2(1+\nu))$
Backfill soil shear wave velocity, V	54 m/s	Calculated from G and γ: $V = (G/(9.81*\gamma))^{1/2}$
Design earthquake magnitude	7.5	Used to calculate displacement from plastic hinging in stem
Design earthquake PGA	0.6 g	Used to check the maximum displacement from hinging
Calculated Results		
Flexural tensile strength concrete, f_t	4.4 MPa	$f_t = 0.75\ f_c^{1/2}$
Cracking moment for stem, M_c	0.090	In dimensionless form ($M_c/\gamma H^3$). Plane strain model
Flexural capacity of stem, M_u	0.135	In dimensionless form ($M_u/\gamma H^3$)
Wall inertia moment at PGA, M_w	0.032	In dimensionless form ($M_w/\gamma H^3$)
Young's modulus concrete, E_c	28 GPa	$E_c = 4700\ f_c^{1/2}$
Moment of inertia for stem	0.0013m^3	Based on uncracked section
Cracking stiffness reduction factor	0.25	Based on Priestley et al, 1996 for cracked columns
Flexibility ratio uncracked stem, d_{wu}	4.2	Equation (1)
Flexibility ratio cracked stem, d_{wc}	16.8	Equation (1)
Backfill active pressure coeff, K_A	0.26	From soil friction angle. Smooth wall.
MO active pressure coefficient, K_{AE}	0.87	For PGA (C_o = 0.60)
Active pressure gravity moment	0.045	In dimensionless form
Stiff wall gravity moment	0.06	Figure 16 (d_w = 4.2). In dimensionless form
Uncracked wall 1-g EQ moment	0.28	Figure 11 (d_w = 4.2). In dimensionless form for C_o = 1.0
Cracked wall 1-g EQ moment	0.16	Figure 11 (d_w = 16.8). In dimensionless form for C_o = 1.0
Top deflection: 1-g EQ, cracked	0.50	Figure 14 (d_w = 16.8). In dimensionless form for C_o = 1.0 $u_t\ G/(C_o\gamma H^2)$: where u_t = top deflection
Top deflection: gravity, cracked	0.01	Figure 14 (d_w = 16.8). In dimensionless form

Moments at the base of the flood channel wall stem and the deflection of the top of the wall are plotted over the design range of the acceleration coefficient (0 to 0.6) in Figure 19. The inertia moment from the wall stem has been added to the combined gravity and earthquake moments (G + E moments). This is a conservative approximation as the "free" inertia load from the wall will be reduced by interaction with the backfill.

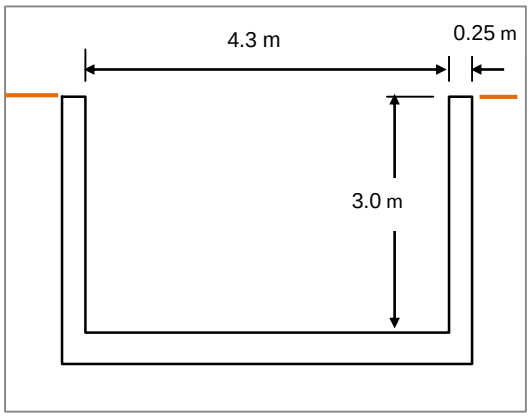

Figure 18. Flood control channel section.

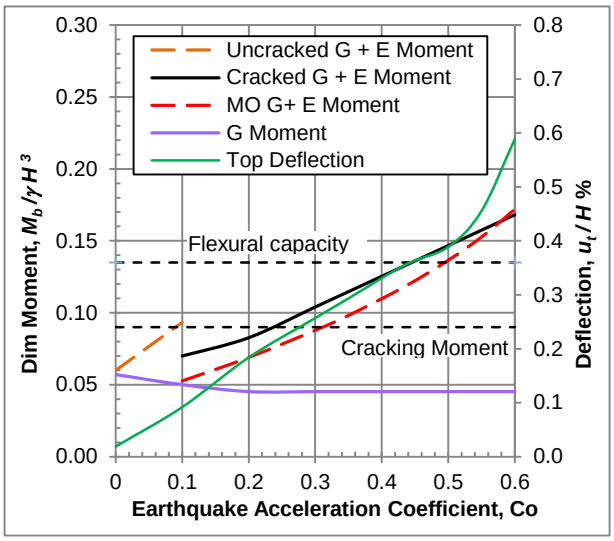

Figure 19. Moment and deflection performance.

The performance curves show that the wall becomes cracked at an acceleration coefficient of 0.1 and reaches its flexural capacity at an acceleration coefficient of 0.43. Over this range, the G + E base moment is approximately 13% greater than the base moment calculated using MO. After the flexural capacity is reached, the wall will deform plastically with rotation at a plastic hinge at the base of the wall. Outward displacement beyond the critical acceleration coefficient of 0.43 was estimated using the Newmark, 1965 sliding block theory and adopting the Jibson, 2007 correlation equation for a displacement probability of exceedance of 16 %. A top displacement of approximately 0.6% of the wall height was estimated at the design acceleration coefficient level of 0.6 indicating a displacement ductility demand on the wall of less than 2. This is a low demand compared to the ductility capacity of approximately five estimated from consideration of strain limits in the stem base.

8 CONCLUSIONS

The flexibility of a retaining wall has a significant influence on the earthquake-induced soil pressures. Methods of predicting earthquake pressures on rigid and flexible walls are well documented in the literature but there is limited published information on the analysis of stiff walls with flexibility intermediate between these limiting cases. Were the wall geometry is relatively simple, the charts presented in this study should provide a convenient preliminary design method for stiff walls and also give an indication of whether significant nonlinear soil behaviour is likely and whether a more sophisticated finite element analysis is justified.

The assumptions made regarding a rigid base and uniform body forces to represent the earthquake load are expected to be conservative in many applications and this needs consideration in design.

9 REFERENCES

Jibson, R W. (2007). Regression Models for Estimating Coseismic Landslide Displacement. *Engineering Geology*, Vol 91, Issues 2-4, pp. 209-218.

Mononobe, N. and Matsuo, H. (1929). On the Determination of Earth Pressures During Earthquakes, *Proc World Eng Conf 9*: 177-185.

Priestley, M.J.N, Calvi G M and Kowalsky M J. (2007). Displacement-Based Seismic Design of Structures, *IUSS Press*.

Veletsos, A.S. and Younan, A.H. (1997). Dynamic Response of Cantilever Retaining Walls. *Journal Geotechnical and Geoenvironmental Engineering, ASCE*, 123, 2, 161-172.

Wood, J.H. (1973). Earthquake-Induced Soil Pressures on Structures, Report No. EERL 73-05, Earthquake Eng Research Laboratory, California Institute of Technology, Pasadena.

Wood, J.H. (1991). Earthquake-Induced Soil Pressures on Flexible Retaining Walls. *Proc Pacific Conference on Earthquake Engineering*, New Zealand.